Analytical Estimation of the Equivalent Elastic Compliance Tensor for Fractured Rock Masses

J. P. Yang[1]; W. Z. Chen[2]; G. J. Wu[3]; and D. S. Yang[4]

Abstract: The elastic compliance matrix is a key parameter for the stability analysis of engineering projects constructed in fractured rock masses. In this study, the energy equivalence and the superposition methods were used to estimate the elastic compliance matrix of rock masses containing persistent or nonpersistent fractures. For the energy equivalence method, two loading schemes were proposed to obtain the values of S_{16} and S_{26} for nonsymmetric fracture sets. The superposition method was proposed to estimate the compliance matrix of rock mass containing several fracture sets by summing the matrices of intact rock and each single fracture set. For a rock mass containing regular persistent fracture sets, the derived analytical results were consistent with closed-form results. The analytical results were also compared with the results of FEM for a rock mass containing two normally distributed nonpersistent fracture sets. The maximum deviations of the directional Young's modulus, shear modulus, and Poisson's ratio were 7.9, 11.3, and 21.3% respectively. The limitations of the proposed methods are discussed in this paper. **DOI: 10.1061/(ASCE)GM.1943-5622.0001035.**

Author keywords: Rock mass; Nonpersistent fracture; Compliance matrix; Strain energy; Superposition.

Introduction

In the analysis of engineering problems dealing with rock masses, the influence of fractures should be considered because the strength and deformation properties of rock masses depend on both the properties of the rock material (i.e., the continuous units of rock) and those of the various structural geological features, specifically, joints and fractures (Brady and Brown 2013). For highly fractured rock mass, in which the fracture spacing is relatively small compared to the structure scale, it is more convenient and practical to treat the fractured rock mass as equivalent continuum material. In addition to the in situ measurements (Bieniawski 1978), empirical relationships (Palmström and Singh 2001; Barton 2002; Sonmez et al. 2004; Zhang and Einstein 2004; Hoek and Diederichs 2006), and numerical methods (Kulatilake et al. 1993; Min and Jing 2003; Esmaieli et al. 2010; Chen et al. 2012; Gutierrez and Youn 2015) in determining the effective elastic modulus of fractured rock mass, analytical solutions have attracted intensive attention because they are concise, clear, and straightforward.

[1]Associate Professor, State Key Laboratory of Geomechanics and Geotechnical Engineering, Institute of Rock and Soil Mechanics, Chinese Academy of Science, Wuhan 430071, China. E-mail: jpyang@whrsm.ac.cn

[2]Professor, State Key Laboratory of Geomechanics and Geotechnical Engineering, Institute of Rock and Soil Mechanics, Chinese Academy of Science, Wuhan 430071, China; Professor, Research Centre of Geotechnical and Structural Engineering, Shandong Univ., Jinan 250061, China. E-mail: wzchen@whrsm.ac.cn

[3]Associate Professor, State Key Laboratory of Geomechanics and Geotechnical Engineering, Institute of Rock and Soil Mechanics, Chinese Academy of Science, Wuhan 430071, China. E-mail: gjwu@whrsm.ac.cn

[4]Professor, State Key Laboratory of Geomechanics and Geotechnical Engineering, Institute of Rock and Soil Mechanics, Chinese Academy of Science, Wuhan 430071, China (corresponding author). E-mail: dsyang@whrsm.ac.cn

Note. This manuscript was submitted on December 14, 2016; approved on July 19, 2017; published online on October 27, 2017. Discussion period open until March 27, 2018; separate discussions must be submitted for individual papers. This paper is part of the ***International Journal of Geomechanics***, © ASCE, ISSN 1532-3641.

The equivalent elastic compliance matrix of rock mass is often derived through two frameworks: the energy equivalence method and strain average method. The energy equivalence method is based on linear elastic fracture mechanics, and it calculates the change of strain energy due to the presence of fractures by taking into account the energy-release rate related to the propagation of a crack and the crack tip stress intensity factor. Because the fractured rock mass at the representative elementary volume (REV) scale is considered as an equivalent continuum material, the elastic-strain energy of the material can be determined using the principle of continuum mechanics, and it will be compared with the total energy obtained from fracture mechanics to estimate the effective moduli or the compliance matrix (Budiansky and O'Connell 1976; Kemeny and Cook 1986; Huang et al. 1995). For the strain average method, the compliance tensor of fractured rock mass is divided into two parts: one relates to the compliance of intact rock without any fracture, and the other is a correction term taking into account the influence of fractures; the second part is called *crack compliance matrix* as in Horii and Nemat-Nasser (1983). The crack compliance matrix is estimated by averaging the strain of a REV for which the evaluation of the relative displacement jumps across the fractures is required (Horii and Nemat-Nasser 1983; Oda et al. 1984).

To calculate the fracture-induced energy increment or the fracture displacement jump, different displacement models of persistent and nonpersistent fractures were adopted. Fig. 1 shows persistent and nonpersistent joints (Kim et al. 2007). For persistent fractures the normal stiffness and shear stiffness of fractures were incorporated to represent the compressive resistance and shear resistance, respectively. As a result, the model can be used to estimate the approximate elastic parameters for persistent rock masses under compression. Huang et al. (1995), Amadei and Goodman (1981), Li (2001), Agharazi et al. (2012) introduced some analytic results based on the persistent fracture model. Furthermore, Wang and Huang (2009) studied the failure mode and simulate the complete prepeak and postpeak deformation of rock mass with sets of persistent joints in three dimensions. For the nonpersistent fractures contained in rock masses, the fractures are often assumed open (traction-free fractures in which the fracture stiffness is zero) (Budiansky and O'Connell 1976; Kemeny and Cook 1986; Hu and

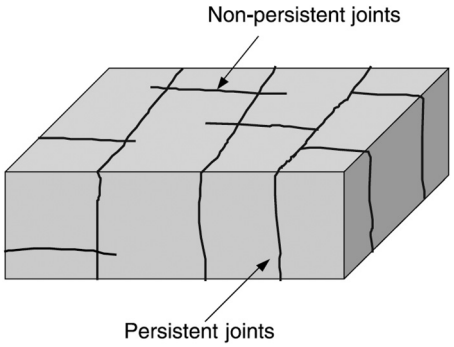

Fig. 1. Illustration of joint persistency (reprinted from *Rock Mechanics and Rock Engineering*, "Estimation of Block Sizes for Rock Masses with Non-Persistent Joints," 40, 2007, 169-192, B. H. Kim, M. Cai, P. K. Kaiser, and H. S. Yang, © Springer-Verlag 2006 with permission of Springer)

Huang 1993) or closed (incompressible fractures in which fracture stiffness is infinitely great) (Horii and Nemat-Nasser 1983; Kachanov 1982; Cai and Horii 1992). For example, Budiansky and O'Connell (1976) and Kemeny and Cook (1986) obtained equivalent elastic moduli for isotropically distributed open cracks using the energy equivalence method. Horii and Nemat-Nasser (1983) found the same result in terms of the mean displacement jumps of open cracks, and they studied the load-induced anisotropy of elastic moduli by considering the closure effects and slip friction of the crack surfaces. For nonpersistent fractures, few analytical studies (Oda et al. 1984) took into account the fracture stiffness despite it being considered one of the most important parameters affecting rock mass properties (Goodman et al. 1968; Bandis et al. 1983). Oda et al. (1984) incorporated the fracture stiffness of nonpersistent fracture to estimate the equivalent compliance matrix within the framework of fabric tensor theory. The displacement jump vector is assumed parallel to the traction vector in Oda et al. (1984). On the basis of fracture mechanics, Yang et al. (2016) proposed a displacement model in which the stiffness of nonpersistent fractures and the influence of the anisotropic elasticity of a rock mass are considered, and they studied the directional equivalent elastic moduli of a fractured rock mass. However, the compliance matrix was not studied in Yang et al. (2016).

In this study, the compliance matrix of a nonpersistent fractured rock mass was derived using both the energy equivalence method and the strain average method by adopting the fracture displacement model proposed in Yang et al. (2016). While using the energy equivalence method, two new loading sets were proposed to determine the values of S_{16} and S_{26} of the compliance matrix. Furthermore, a superposition method was proposed to estimate the compliance matrix that is based on the elementary compliance matrices of intact rock and a single fracture set. The proposed methods were verified by comparing the results with those from the closed-form expressions of a regular fractured rock mass and the FEM numerical results of a nonpersistent fractured rock mass. The performance and limits of the proposed methods are discussed in the final section of the paper.

Components of a Compliance Matrix in Two Dimensions

Following Hooke's law, the strain tensor, ε_{ij}, is related to the stress tensor, σ_{kl}, through an elastic compliance tensor, S_{ijkl}, as

$$\varepsilon_{ij} = S_{ijkl}\sigma_{kl}(i,j,k,l = 1,2) \tag{1}$$

Eq. (1) can be written in the following matrix form:

$$\begin{Bmatrix} \varepsilon_{xx} \\ \varepsilon_{yy} \\ \cancel{\varepsilon_{zz}} \\ \cancel{\varepsilon_{yz}} \\ \cancel{\varepsilon_{xz}} \\ \varepsilon_{xy} \end{Bmatrix} = \begin{pmatrix} S_{11} & S_{12} & \cancel{S_{13}} & \cancel{S_{14}} & \cancel{S_{15}} & S_{16} \\ S_{21} & S_{22} & \cancel{S_{23}} & \cancel{S_{24}} & \cancel{S_{25}} & S_{26} \\ \cancel{S_{31}} & \cancel{S_{32}} & \cancel{S_{33}} & \cancel{S_{34}} & \cancel{S_{35}} & \cancel{S_{36}} \\ \cancel{S_{41}} & \cancel{S_{42}} & \cancel{S_{43}} & \cancel{S_{44}} & \cancel{S_{45}} & \cancel{S_{46}} \\ \cancel{S_{51}} & \cancel{S_{52}} & \cancel{S_{53}} & \cancel{S_{54}} & \cancel{S_{55}} & \cancel{S_{56}} \\ S_{61} & S_{62} & \cancel{S_{63}} & \cancel{S_{64}} & \cancel{S_{65}} & S_{66} \end{pmatrix} \begin{Bmatrix} \sigma_{xx} \\ \sigma_{yy} \\ \cancel{\sigma_{zz}} \\ \cancel{\tau_{yz}} \\ \cancel{\tau_{xz}} \\ \tau_{xy} \end{Bmatrix} \tag{2}$$

As is well-known, for any two-dimensional (2D) plane stress problem, the stresses σ_{zz}, τ_{yz}, and τ_{xz} are 0. Therefore, if the conjugate strains ε_{zz}, ε_{yz}, and ε_{xz} are not of interest, components in the third, fourth, and fifth rows and columns of the compliance matrix in Eq. (2) can be removed. For plane-strain problems, the components in the third row and column of the matrix should be determined (Min and Jing 2003).

The "engineering" shear strains (e.g., γ_{xy}) are usually used in Eq. (2), and the compliance matrix is symmetric. In the present study, shear strains (e.g., ε_{xy}) were used to keep the tensor characteristics of the strain components and to facilitate the transformation of compliance matrix in different coordinate systems. Use of shear strains indicates that $S_{12} = S_{21}$, $S_{16} = 2S_{61}$ and $S_{26} = 2S_{62}$. Therefore, only six components in Eq. (2) (S_{11}, S_{22}, S_{12}, S_{16}, S_{26}, and S_{66}) need to be determined.

Methods of Compliance Matrix Determination

Energy Equivalence Method

Estimation of Elastic-Strain Energy

A convenient basis for studying the effect of fractures on the moduli of a rock mass is to consider the stored elastic-strain energy. If an homogeneous and isotropic elastic body with a volume V is subjected to a stress σ_{ij}, then the elastic energy stored in the intact body is U_0V, where U_0 is the elastic-strain energy density of the intact body. For fractures introduced into the body, the total elastic-strain energy will increase by an increment from U_0V to $U_0V + \Delta\Sigma(\text{fractures})$. Then the total elastic-strain energy density, U, stored in the elastic body with fractures can be written as

$$U = U_0 + \sum_{i=1}^{N} \rho_i \Delta\Sigma_i \tag{3}$$

where N = number of fracture sets; ρ_i = fracture density of the ith fracture set, defined as the number of fracture central points per square meter for a 2D problem; and $\Delta\Sigma_i$ = increment of strain energy due to the presence of a single fracture of the ith fracture set. In general, the energy for a given fracture or fracture set depends on the presence or absence of other fracture sets because the other fracture sets alter the overall elastic properties.

Furthermore, the elastic-strain energy density stored in the described equivalent continuum material on the REV scale can be determined with Eq. (4); however, the determination of the REV is beyond of the scope of this study. Eq. (4) is written as

$$\bar{U} = \frac{1}{2}\sigma_{ij}\varepsilon_{ij} \tag{4}$$

By equating Eqs. (3) and (4), the components in the equivalent compliance matrix in Eq. (2) can be determined. The key step is calculating the strain-energy change, $\Delta\Sigma_i$, in Eq. (3).

For an open fracture, Irwin (1957) argued that the strain-energy increment (denoted as $\Delta\Sigma$) due to a single fracture can be estimated using the energy-release rate; this method was adopted by Kemeny and Cook (1986) and Hu and Huang (1993) to derive the effective moduli of a rock mass containing open fractures. However, if fracture stiffness cannot be neglected, the deformation of fractures are restrained because of fracture resistance, and the strain energy is changed. The strain-energy change of a single fracture is calculated by considering the additional strain energy in the fracture and in the surrounding rock. The additional strain energy in a fracture is estimated by multiplying the fracture stiffness and the fracture displacement. In a similar manner, multiplying the stress acting on a fracture surface by the fracture displacement, the additional strain energy in surrounding rock is estimated.

The strain-energy increment is expressed as $\Delta\Sigma = \Delta\Sigma_{rn} + \Delta\Sigma_{fn} + \Delta\Sigma_{rs} + \Delta\Sigma_{fs}$, where $\Delta\Sigma_{rn}$ and $\Delta\Sigma_{fn}$ are the additional elastic-strain energy in the rock and fracture, respectively, due to the resolved normal stress, and $\Delta\Sigma_{rs}$ and $\Delta\Sigma_{fs}$ are the additional elastic-strain energy in the rock and fracture, respectively, due to the resolved shear stress. The strain energy is firmly related to the normal stiffness, K_n, and the shear stiffness, K_s, of rock fracture. By assuming uniform displacement jumps along fracture, Yang et al. (2016) argued that the normal displacement jump, δ_n, and shear displacement jump, δ_s, can be determined using Eqs. (5*a*) and (5*b*), respectively. When the fracture stiffness decreases to zero, the displacement jump equals the average value for the open fractures. From Eq. (5), the strain-energy change in the rock and fracture can be obtained by Eq. (6) (Yang et al. 2016). It is noteworthy that the coupling effects between normal (shear) stresses and shear (normal) displacements of fractures are ignored. Eqs. (5*a*), (5*b*), and (6) are written as

$$\delta_n = \frac{\pi a}{K_n \pi a + E_\perp}\sigma_n \tag{5a}$$

$$\delta_s = \frac{\pi a}{K_s \pi a + E_\parallel}\tau_s \tag{5b}$$

$$\Delta\Sigma = \frac{\pi a^2}{K_n \pi a + E_\perp}\cdot\sigma_n^2 + \frac{\pi a^2}{K_s \pi a + E_\parallel}\cdot\tau_s^2 \tag{6}$$

where a = half-length of fracture; σ_n and τ_s = normal and shear stress acting on a fracture surface; and $E_\perp$ and $E_\parallel$ = effective elastic moduli of a rock mass in the normal and shear directions of the fracture, respectively. If the interaction between neighboring fractures is neglected, $E_\perp$ and $E_\parallel$ are replaced by the Young's modulus of the intact, unfractured material, E_0.

To determine the compliance matrix of rock mass containing N fracture sets, the directional elastic moduli $(E_{\perp 1}, E_{\parallel 1}), \ldots, (E_{\perp N}, E_{\parallel N})$ in Eq. (6) need to be estimated first.

If a far-field uniaxial stress, σ, is applied, then Eq. (3) can be written as

$$\frac{\sigma^2}{2E} = \frac{\sigma^2}{2E_0} + \sum_{i=1}^{N}\rho_i\Delta\Sigma_i \tag{7}$$

where E = overall Young's modulus in the loading direction of the fractured material, which is determined by the Young's modulus of the uncracked material and by the characteristics of the cracks.

By substituting Eq. (6) into Eq. (7) and resolving the far-field stress, σ, into normal stress, σ_n, and shear stress, τ_s, on the fracture surface, the directional elastic moduli can be estimated through Eq. (8). It is noteworthy that the stress acting on the fracture surface resolved from far-field stress is a rough approximation and can be accepted in the homogenization sense. The presence of fractures could magnify or shield the local stress around the fractures. Eq. (8) is written as

$$\frac{1}{E} = \frac{1}{E_0} + \frac{1}{2}\sum_{i=1}^{N}\rho_i\cdot\left[\frac{\pi a_i^2(1+\cos 2\theta_i)^2}{K_n\pi a_i + E_{\perp i}} + \frac{\pi a_i^2\sin^2 2\theta_i}{K_s\pi a_i + E_{\parallel i}}\right] \tag{8}$$

where θ_i = angle between the loading and normal directions of fracture surface; θ_i = one-half the length of fracture; and $E_{\perp i}$ and $E_{\parallel i}$ = elastic moduli in directions perpendicular and parallel, respectively, to the plane of the ith fracture set.

For a rock mass containing N fracture sets, there are $2N$ unknowns in Eq. (8); that is, $E_{\perp 1}, E_{\parallel 1}, \ldots, E_{\perp N}, E_{\parallel N}$. By applying the far-field stress, σ, in $2N$ specific directions (parallel and perpendicular to the N fractures sets), $2N$ equations can be set up from Eq. (8), and the directional elastic modulus on the left side of Eq. (8) is then just the specific directional elastic modulus $(E_{\perp 1}, E_{\parallel 1}, \ldots, E_{\perp N}, E_{\parallel N})$. Thus, the $2N$ unknowns of $E_{\perp 1}, E_{\parallel 1}, \ldots, E_{\perp N}, E_{\parallel N}$ can be solved from $2N$ independent equations.

Similarly, if a far-field shear stress, τ, is applied, Eq. (3) can be written as

$$\frac{\tau^2}{2G} = \frac{\tau^2}{2G_0} + \sum_{i=1}^{N}\rho_i\Delta\Sigma_i \tag{9}$$

Following the same procedure, the shear modulus can be expressed as follows:

$$\frac{1}{G} = \frac{1}{G_0} + 2\sum_{i=1}^{N}\rho_i\cdot\left(\frac{\pi a_i^2\sin^2 2\theta_i}{K_n\pi a_i + E_{\perp i}} + \frac{\pi a_i^2\cos^2 2\theta_i}{K_s\pi a_i + E_{\parallel i}}\right) \tag{10}$$

Determination of the Unknown Components in a Compliance Matrix

In numerical studies, three independent boundary conditions, such as Loading Sets 1–3 shown in Fig. 2, are enough to determine the six unknown components of the 2D compliance matrix of an anisotropic elastic body (Min and Jing 2003; Khani et al. 2013; Yang et al. 2014). More boundary conditions, such as Loading Sets 4 and 5 in Fig. 2, are unnecessary. Strains of the other loading conditions can be obtained through superposition of the strain results of Loading Sets 1–3 because of the linear relationships between strains and stresses in Eq. (2). However, three boundary conditions are not enough for an analytical study using the energy equivalence method because only one independent equation can be set up for each loading setup. The relationship between the elastic-strain energy and the stress components is not linear [e.g., Eq. (6)]. Therefore, the elastic-strain energy in other loading sets is not a superposition of the strain energy of Loading Sets 1–3. Hu and Huang (1993) used four loading sets to determine the four in-plane elastic constants for symmetric fracture distributions. For rock masses in which the fracture distribution is not symmetric, shear stress induces the variation of normal strain and vice versa. Therefore, additional loading schemes were used to estimate the values of S_{16} and S_{26}. A previous numerical study showed that S_{16} and S_{26} can significantly influence the directional elastic moduli of rock masses, and the neglect of S_{16} and S_{26} leads to incorrect results [Fig. 4 in Yang et al. (2014)]. In the present study, two new loading schemes, Loading Sets 5 and 6, in Fig. 2, were proposed to determine S_{16} and S_{26}.

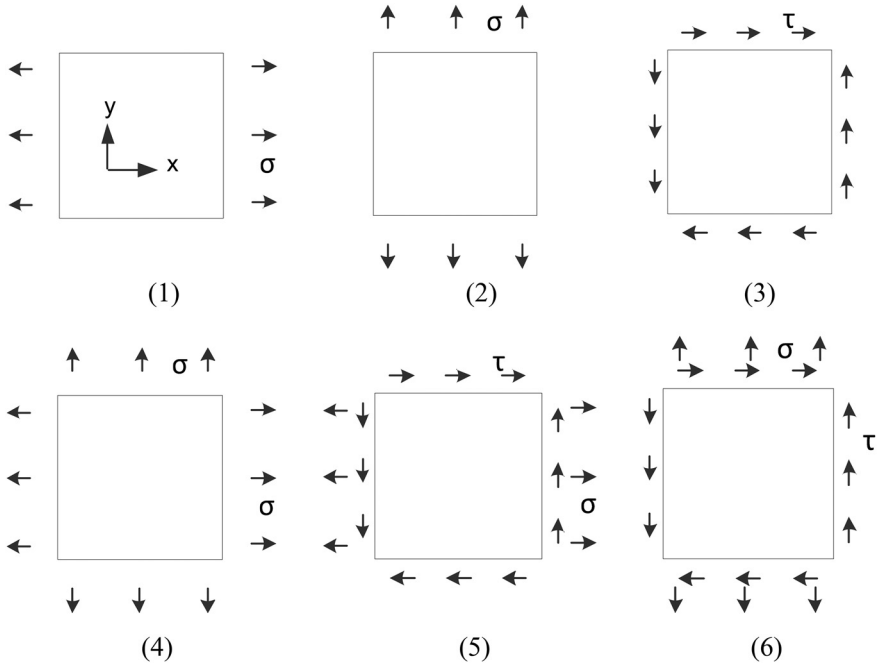

Fig. 2. Six loading sets for determining the six unknown components of the compliance matrix for 2D anisotropic material

The elastic-strain energy density stored in the fractured body can be estimated from Eqs. (6), (7), and (9). The energy density can also be obtained through Eq. (4) by considering the fractured body as an equivalent elastic material. Using the elastic-strain energy density formulas and activating different loading sets, the components of the compliance matrix can be determined and the results expressed, as in Eqs. (11)–(16) (see Appendix for details), which are written as

$$S_{11} = \frac{1}{E_0} + \frac{1}{2}\sum_{i=1}^{N} \rho_i \pi a_i^2 \cdot \left[\frac{(1+\cos 2\theta_{ix})^2}{K_n \pi a_i + E_{\perp i}} + \frac{\sin^2 2\theta_{ix}}{K_s \pi a_i + E_{\parallel i}} \right] \tag{11}$$

$$S_{22} = \frac{1}{E_0} + \frac{1}{2}\sum_{i=1}^{N} \rho_i \pi a_i^2 \cdot \left[\frac{(1-\cos 2\theta_{ix})^2}{K_n \pi a_i + E_{\perp i}} + \frac{\sin^2 2\theta_{ix}}{K_s \pi a_i + E_{\parallel i}} \right] \tag{12}$$

$$S_{66} = \frac{1}{2G_0} + \sum_{i=1}^{N} \rho_i \pi a_i^2 \cdot \left(\frac{\sin^2 2\theta_{ix}}{K_n \pi a_i + E_{\perp i}} + \frac{\cos^2 2\theta_{ix}}{K_s \pi a_i + E_{\parallel i}} \right) \tag{13}$$

$$S_{12} = -\frac{\nu_0}{E_0} - \frac{1}{2}\sum_{i=1}^{N} \rho_i \pi a_i^2 \cdot \left(\frac{\sin^2 2\theta_{ix}}{K_s \pi a_i + E_{\parallel i}} - \frac{\sin^2 2\theta_{ix}}{K_n \pi a_i + E_{\perp i}} \right) \tag{14}$$

$$S_{16} = \sum_{i=1}^{N} \rho_i \pi a_i^2 \cdot \left[\frac{(1+\cos 2\theta_{ix}) \cdot \sin 2\theta_{ix}}{K_n \pi a_i + E_{\perp i}} - \frac{\cos 2\theta_{ix} \cdot \sin 2\theta_{ix}}{K_s \pi a_i + E_{\parallel i}} \right] \tag{15}$$

$$S_{26} = \sum_{i=1}^{N} \rho_i \pi a_i^2 \cdot \left[\frac{(1-\cos 2\theta_{ix}) \cdot \sin 2\theta_{ix}}{K_n \pi a_i + E_{\perp i}} + \frac{\cos 2\theta_{ix} \cdot \sin 2\theta_{ix}}{K_s \pi a_i + E_{\parallel i}} \right] \tag{16}$$

To summarize, there are a total of $2N + 6$ unknowns, consisting of the $2N$ directional moduli $\left(E_{\perp 1}, E_{\parallel 1}, \ldots, E_{\perp N}, E_{\parallel N}\right)$ that appear in Eq. (8), and the six compliance parameters, S_{ij}, that appear in Eqs. (11)–(16). There are also, therefore, $2N + 6$ equations. The compliance parameters, S_{ij}, depend on the coordinate frame, and it is straightforward to confirm that, because of the inclusion of the angular terms on the right sides of Eqs. (11)–(16), these parameters do transform in the appropriate manner between coordinate frames.

Strain Average Method

The compliance matrix is also obtained using the strain average method, which focuses on the fracture-induced strain.

General Formulation

For an elastic body containing fractures, the equivalent compliance matrix, S_{ijkl}, in Eq. (1) can be thought of as consisting of two parts: The first, M_{ijkl}, depends on the elasticity of the matrix without any cracks, while the second, C_{ijkl}, represents the correction part related to the existing fractures. The relationship is written as

$$S_{ijkl} = M_{ijkl} + C_{ijkl} \tag{17}$$

Using the divergence theorem, Horii and Nemat-Nasser (1983) proved that C_{ijkl} satisfies

$$C_{ijkl}\sigma_{kl} = \frac{1}{V}\int_{2S} \frac{1}{2}(u_i n_j + u_j n_i) \mathrm{dS} \tag{18}$$

where V = total volume of the cracked body; $2S$ = total surface area of all fractures; u_i and u_j = components of a displacement vector; and n_i and n_j = components of a unit vector normal to the crack surfaces.

For each single rectilinear fracture, n_i and n_j are constant along each surface. Hence, using the displacement jumps, Eq. (18) can be expressed as

$$C_{ijkl}\sigma_{kl} = \frac{1}{2V}\sum_{n=1}^{m^{(V)}} S^{(n)}(\delta_i n_j + \delta_j n_i) \tag{19}$$

where $m^{(V)}$ = number of cracks in the studied body V; and $S^{(n)}$ = area of the nth crack. (A kth crack among the $m^{(V)}$ cracks consists of two surfaces having the same area of $S^{(k)}$.)

Determination of the Unknown Components in a Compliance Matrix

To express the term $\delta_i n_j + \delta_j n_i$ in Eq. (19), two coordinate systems were defined and are shown in Fig. 3. The rotation matrix, $[\alpha]$, was used to translate δ_n, δ_s ($\delta_n = \delta_{1'}, \delta_s = \delta_{2'}$ in the local coordinate system) to δ_i, δ_j in the global coordinate system. The rotation matrix, $[\beta]$, was used to express σ_n, τ_s ($\sigma_n = \sigma_{1'1'}, \tau_s = \sigma_{1'2'}$) in Eqs. (5*a*) and (5*b*) from σ_{ij} in a global coordinate system. $[n]$ denotes the unit normal vector of fracture surface.

$$[\alpha] = [\alpha_{im'}] = [\alpha_{jm'}] = \begin{bmatrix} \alpha_{11'} & \alpha_{12'} \\ \alpha_{21'} & \alpha_{22'} \end{bmatrix} = \begin{bmatrix} \cos\theta & -\sin\theta \\ \sin\theta & \cos\theta \end{bmatrix} \tag{20}$$

$$[\beta] = [\beta_{i'k}] = [\beta_{i'l}] = \begin{bmatrix} \beta_{1'1} & \beta_{1'2} \\ \beta_{2'1} & \beta_{2'2} \end{bmatrix} = \begin{bmatrix} \cos\theta & \sin\theta \\ -\sin\theta & \cos\theta \end{bmatrix} \tag{21}$$

$$[n] = [n_i] = \begin{bmatrix} n_1 \\ n_2 \end{bmatrix} = \begin{bmatrix} \cos\theta \\ \sin\theta \end{bmatrix} \tag{22}$$

From the displacement jumps of fracture [Eqs. (5*a*) and (5*b*)], the term $\delta_i n_j + \delta_j n_i$ in Eq. (19) becomes

$$\begin{aligned} \delta_i n_j + \delta_j n_i &= n_i\alpha_{jm'}\delta_{m'} + n_j\alpha_{im'}\delta_{m'} = (n_i\alpha_{j1'} + n_j\alpha_{i1'})\delta_{1'} \\ &+ (n_i\alpha_{j2'} + n_j\alpha_{i2'})\delta_{2'} = \frac{\pi a}{K_n\pi a + E_\perp}(n_i\alpha_{j1'} + n_j\alpha_{i1'})\sigma_n \\ &+ \frac{\pi a}{K_s\pi a + E_\parallel}(n_i\alpha_{j2'} + n_j\alpha_{i2'})\tau_s \\ &= \left[\frac{\pi a}{K_n\pi a + E_\perp}(n_i\alpha_{j1'} + n_j\alpha_{i1'})\beta_{1'k}\beta_{1'l}\right. \\ &+ \left.\frac{\pi a}{K_s\pi a + E_\parallel}(n_i\alpha_{j2'} + n_j\alpha_{i2'})\beta_{1'k}\beta_{2'l}\right]\sigma_{kl} \end{aligned} \tag{23}$$

For a rock mass containing N sets of regular fractures, substitution of Eq. (23) into Eq. (19), and cancellation of the stress term, gives

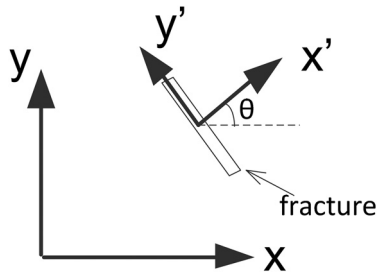

Fig. 3. Global coordinate system xy and local coordinate system $x'y'$

$$C_{ijkl} = \sum_{m=1}^{N} \rho_m \pi a_m^2 \cdot \left[\frac{(n_i\alpha_{j1'} + n_j\alpha_{i1'})\beta_{1'k}\beta_{1'l}}{K_n\pi a_m + E_{\perp m}} + \frac{(n_i\alpha_{j2'} + n_j\alpha_{i2'})\beta_{1'k}\beta_{2'l}}{K_s\pi a_m + E_{\parallel m}}\right] \tag{24}$$

Substituting the terms of n_i, $\alpha_{ij'}$, and $\beta_{i'j}$ [in Eqs. (20)–(22)] into Eq. (24), the values of C_{1111}, C_{2222}, $C_{1212} + C_{1221}$, C_{1122}, $C_{1112} + C_{1121}$, and $C_{2212} + C_{2221}$ are equal to the corresponding terms of S_{11}, S_{22}, S_{66}, S_{12}, S_{16}, and S_{26} in Eqs. (11)–(16).

Superposition Method

The equivalent compliance tensor of a rock mass containing N fracture sets can be considered as the approximate sum of the individual equivalent compliance tensors of intact rock, Fracture Set 1, Fracture Set 2,…, Fracture Set N. For each fracture set, the elementary compliance matrix in the local coordinate system is transformed to the compliance matrix in the global coordinate system. It is noteworthy that the interaction between different fracture sets is ignored in this case. Kachanov (1993) stated that when the fracture centers are randomly distributed, the competing effects of shielding and amplification (of stress due to neighboring fractures) may be balanced and cancel each other, even at high fracture densities. In addition, for at least two orientation statistics—parallel and randomly oriented fractures—the results were confirmed. Hence, the approximation of noninteracting fractures remains accurate.

For example, for a fractured rock mass containing three sets of persistent fractures (Fig. 4), the equivalent compliance matrix can be obtained by summing the individual compliance matrices in the global coordinate system. According to the results of Amadei and Goodman (1981), the elementary compliance matrix of one set of persistent fractures can be expressed as

$$S_{\text{persistent}} = \begin{pmatrix} 0 & & & & & \\ & \frac{1}{K_n S} & & & & \\ & & 0 & & & \\ & & & \frac{1}{2K_s S} & & \\ & & & & 0 & \\ & & & & & \frac{1}{2K_s S} \end{pmatrix} \tag{25}$$

In Fig. 4, S'_{set2} and S'_{set3} are the compliance matrices in the local system $x'y'$ and follow the same form as S_{set1}. T is the transformation matrix. For a 2D problem, when the local coordinate system $x'y'$ is rotated around the $z'(=z)$ axis with angle θ to the global coordinate system xy ($\theta = -\varphi$ for Set 2 and $\theta = -\pi/2$ for Set 3), T has the following form:

$$[T] = \begin{pmatrix} \cos^2\theta & \sin^2\theta & 0 & 0 & 0 & 2\cos\theta\sin\theta \\ \sin^2\theta & \cos^2\theta & 0 & 0 & 0 & -2\cos\theta\sin\theta \\ 0 & 0 & 1 & 0 & 0 & 0 \\ 0 & 0 & 0 & \cos\theta & -\sin\theta & 0 \\ 0 & 0 & 0 & \sin\theta & \cos\theta & 0 \\ -\cos\theta\sin\theta & \cos\theta\sin\theta & 0 & 0 & 0 & \cos^2\theta - \sin^2\theta \end{pmatrix} \tag{26}$$

For S_1 of 0.5, S_2 of 0.75, and S_3 of 1.5 m and φ of 45°, the directional Young's modulus and shear modulus, determined using the

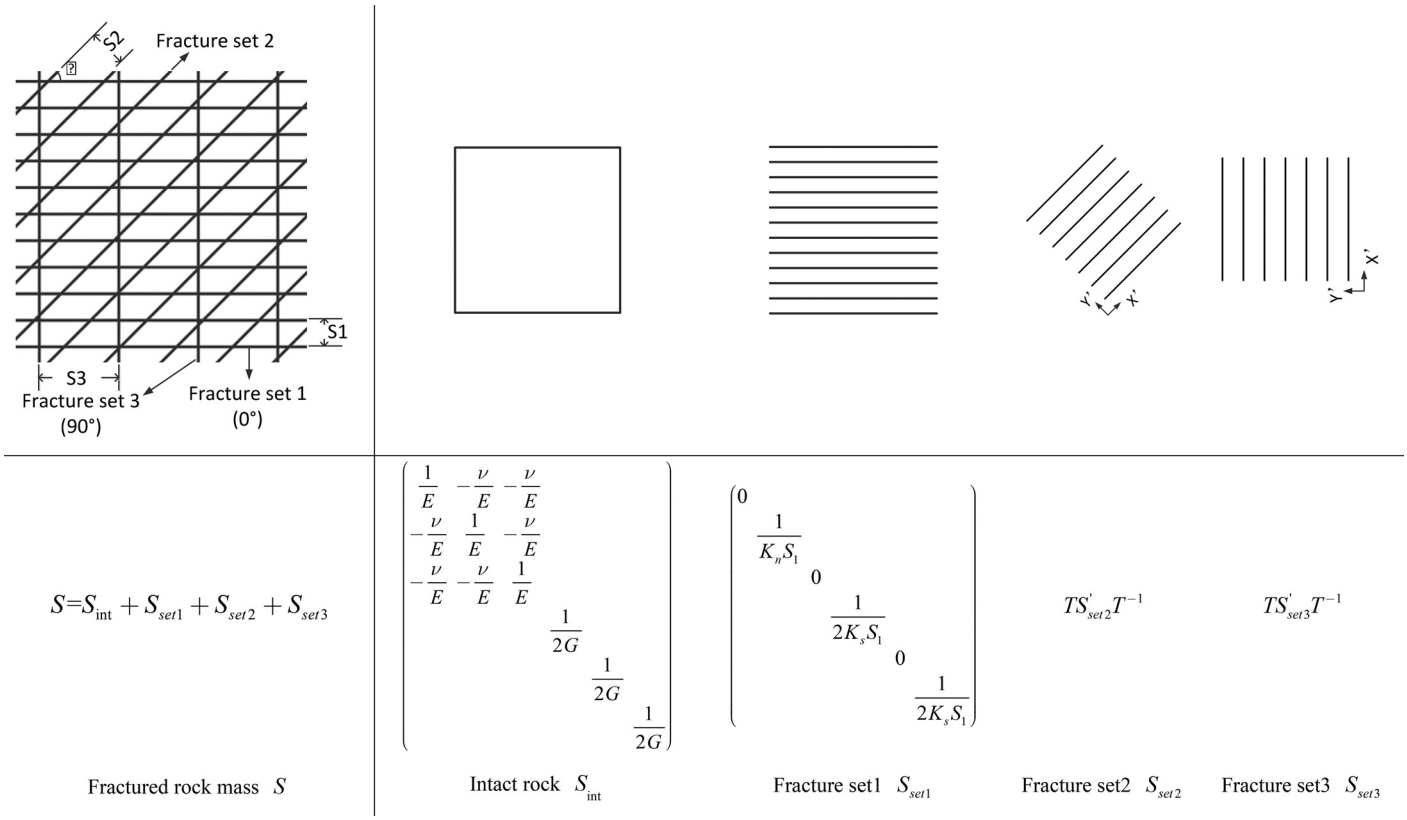

Fig. 4. Determination of the compliance matrix of a fractured rock mass by superposition of each single matrix

superposed compliance matrix (S in Fig. 4) and Eqs. (8) and (10), were plotted and are shown in Fig. 5 to compare the two methods (i. e., the superposition and energy equivalence methods). The fracture densities in Eqs. (8) and (10) were calculated using Eq. (29) for persistent fractures. The results show that the superposition method gave the same results as the energy equivalence method. It can also be seen that the shear modulus in Fig. 5(b) shows near symmetry, but the Young's modulus in Fig. 5(a) does not. The finding implies that the symmetry of Young's modulus may be lost for complex fracture set distribution.

The elementary compliance matrix of one set of nonpersistent fractures (Fig. 6) can be easily determined from Eq. (24) as follows:

$$S_{\text{nonpersistent}}=\begin{pmatrix} 0 & & & & & \\ & \frac{2\rho\pi a^2}{K_n\pi a+E} & & & & \\ & & 0 & & & \\ & & & \frac{\rho\pi a^2}{K_s\pi a+E} & & \\ & & & & 0 & \\ & & & & & \frac{\rho\pi a^2}{K_s\pi a+E} \end{pmatrix} \tag{27}$$

According to the elementary compliance matrices of the nonpersistent fracture set [Eq. (27)] and persistent fracture set [Eq. (25)], the equivalent compliance matrix of rock masses containing several sets of persistent, nonpersistent, or mixed types of fractures can be roughly estimated using the superposition method. This method was used as described in the following section to determine the equivalent compliance matrix of a rock mass containing two sets of nonpersistent fractures.

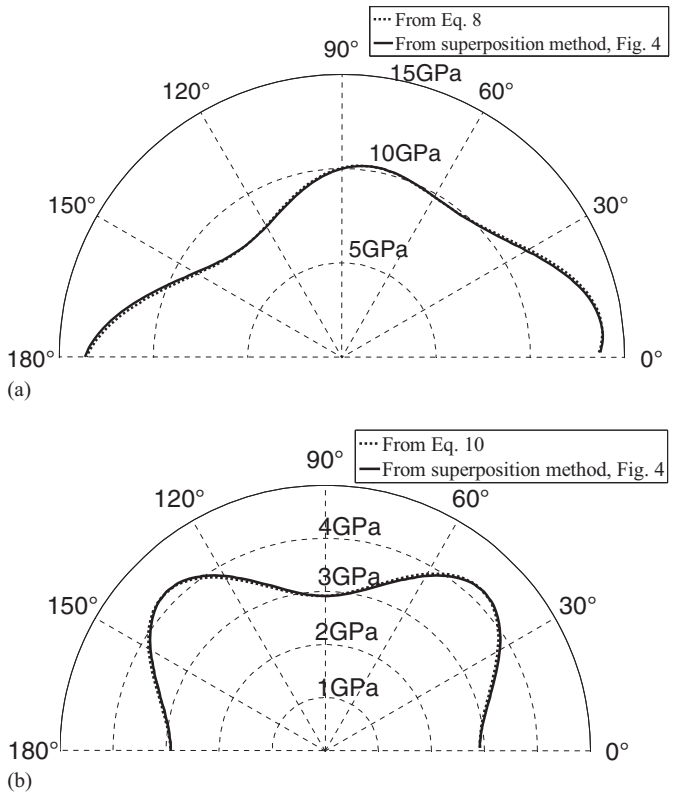

Fig. 5. Comparison of the elastic constants between the superposition method and energy method (in gigapascals): (a) Young's modulus; (b) shear modulus

Eq. (27) was written in three-dimensional (3D) form for matrix transformation. However, it can only be used to evaluate the compliance matrix of 2D plane-stress problems. The displacement formula used in Eq. (24) is only valid for 2D fractures under plane-stress conditions [Eq. (5)]. For plane-strain problems, Young's modulus, E, in Eq. (27) needs to be replaced with $E/(1-\upsilon^2)$.

Verification Using a Closed-Form Solution for Rock Masses with Persistent Fractures

If the fracture length tends to infinity, the expressions in Eqs. (11)–(16) are the results for the special cases of persistent fractures.

Huang et al. (1995) derived a closed-form expression of compliance matrix for a rock mass with three sets of nonorthogonal fractures that are persistent. The angle between the first two sets of joints was γ, and the third set of joints was orthogonal with the first two joint sets. The closed-form solution showed that the third set of joints had no influence on the in-plane elastic constants of the rock mass. When the angle between the first two sets of joints was 90°, the expression became the closed-form solution proposed by Amadei and Goodman (1981) for orthogonal joint sets. The comparison presented in this section focuses on the in-plane elastic constants.

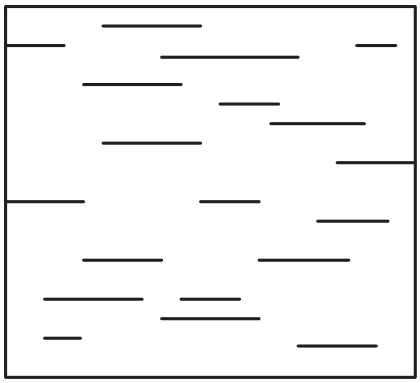

Fig. 6. Schematic map of rock mass containing one set of nonpersistent fractures

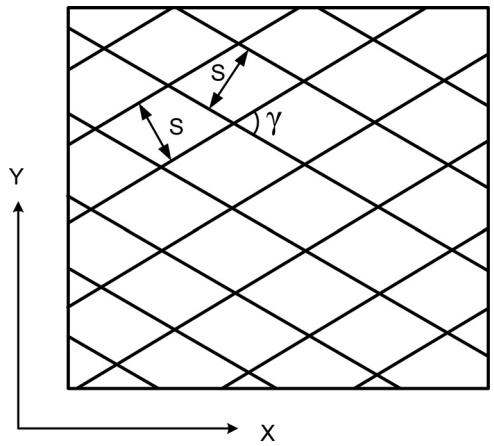

Fig. 7. Schematic map of rock mass with two sets of fractures (adapted from Huang et al. 1995)

Fig. 7 shows the schematic map of the two in-plane intersecting fracture sets. The relationships between θ_{ix}, θ_{iy}, and γ are

$$\theta_{ix} = \frac{\pi}{2} \pm \frac{\gamma}{2},\ \theta_{iy} = \pm \frac{\gamma}{2} \tag{28}$$

For the two fracture sets with spacing S in square L^2, the fracture densities are

$$\rho_i = \frac{L/S}{L^2} = \frac{1}{LS} = \frac{1}{2a_i S} \qquad i = 1, 2 \tag{29}$$

Hence, expressions of S_{11}, S_{22}, S_{12}, S_{16}, and S_{26} in Eqs. (11), (12), and (14)–(16) degenerated as those in Huang et al. (1995) did, but S_{66}, which corresponds to $1/G_{yz}$ in Eq. 14 in Huang et al. (1995), did not. Validating the expression of S_{66} [Eq. (30)] is done by setting φ to 45° and γ to 90°, and the obtained result of S_{66}, as follows, is consistent with the results of Amadei and Goodman (1981):

$$S_{66} = \frac{1}{2G_0} + \sum_{i=1}^{2} \rho_i \pi a_i^2 \cdot \left(\frac{\sin^2 2\theta_{iy}}{K_n \pi a_i + E_{\perp i}} + \frac{\cos^2 2\theta_{iy}}{K_s \pi a_i + E_{\parallel i}} \right) \Bigg|_{a_i \to \infty}$$
$$= \frac{1}{2G_0} + \frac{\sin^2 \gamma}{K_n S} + \frac{\cos^2 \gamma}{K_s S} \tag{30}$$

Comparison with FEM Results for Normally Distributed Nonpersistent Fractures

For a 2D nonpersistent fractured rock mass, the equivalent compliance matrix obtained by FEM modeling (Yang et al. 2014) was used in the present study to compare results from the derived expressions presented in the previous sections. The geometric distribution of fractures used for the FEM modeling, including fracture spacing, dip direction, and fracture trace length, followed normal distribution. Fig. 8 shows the FEM mesh and fracture distribution (long, dark lines). The linear elastic constitutive models are used for an intact rock and fracture. In the present study, the mean values of fracture distribution parameters and the same mechanical parameters for the intact rock and fracture are listed in Table 1. The derived compliance matrices from the energy equivalence method and the strain average method are the same and are written as

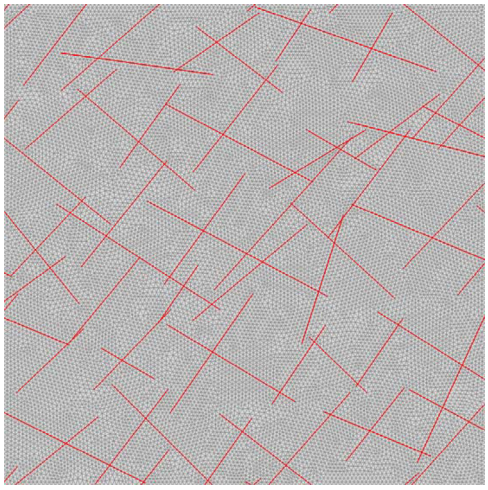

Fig. 8. Generated fracture model of 12-m size mesh for FEM analysis

Table 1. Parameters of Intact Rock and Nonpersistent Fractures

Intact rock		Fractures					
						Stiffness (GPa/m)	
Young's modulus [E_0 (GPa)]	Poisson's ratio (υ_0)	Set	Dip direction (degrees)	Mean trace length (m)	Fracture density (m^{-2})	Normal	Shear
50	0.25	1	150	4	0.16	50	10
		2	50	3	0.25	50	10

$$S = \begin{pmatrix} 44.47 & -20.10 & -5 & 0 & 0 & 8.10 \\ -20.10 & 47.98 & -5 & 0 & 0 & -11.20 \\ -5 & -5 & 20 & 0 & 0 & 0 \\ 0 & 0 & 0 & 0 & 0 & 0 \\ 0 & 0 & 0 & 0 & 0 & 0 \\ 4.05 & -5.60 & 0 & 0 & 0 & 41.99 \end{pmatrix} \times 10^{-12} \ (\text{pa}^{-1}) \tag{31}$$

Using Eq. (27), the derived compliance matrix from the superposition method is

$$S = \begin{pmatrix} 40.46 & -15.43 & -5 & 0 & 0 & 6.07 \\ -15.43 & 43.83 & -5 & 0 & 0 & -8.69 \\ -5 & -5 & 20 & 0 & 0 & 0 \\ 0 & 0 & 0 & 0 & 0 & 0 \\ 0 & 0 & 0 & 0 & 0 & 0 \\ 3.03 & -4.35 & 0 & 0 & 0 & 40.14 \end{pmatrix} \times 10^{-12} \ (\text{pa}^{-1}) \tag{32}$$

The directional elastic constants obtained using the energy equivalence method [Eq. (31)], the superposition method [Eq. (32)], and FEM (Yang et al. 2014) were plotted and are shown in Fig. 9. The results show that the analytical results agreed well with the FEM results. The maximum deviations of the results obtained by the equivalent energy method and the FEM method for Young's modulus, shear modulus, and Poisson's ratio were 5.8, 7.1, and 10.4%, respectively. As the interacting effect of the neighboring fractures is ignored in the superposition method [Eq. (32)], the superposition method predicts larger Young's and shear moduli and a smaller Poisson's ratio than the FEM method and the equivalent energy method [Eq. (31)]. The maximum deviation of the results of Young's modulus, shear modulus, and Poisson's ratio obtained by the superposition method from the FEM are 7.9, 11.3, and 21.3%, respectively. The deviation is acceptable for engineering analysis in practice. The analytical results obtained using the energy equivalence method showed more significant anisotropic characteristics than the results of FEM modeling. This difference can be attributed to the analytical method using the mean geometric data of the fracture sets while the FEM modeling considers the randomness of the distributions of fracture length and the dip angle such that the distribution strengthens the isotropic properties of the material.

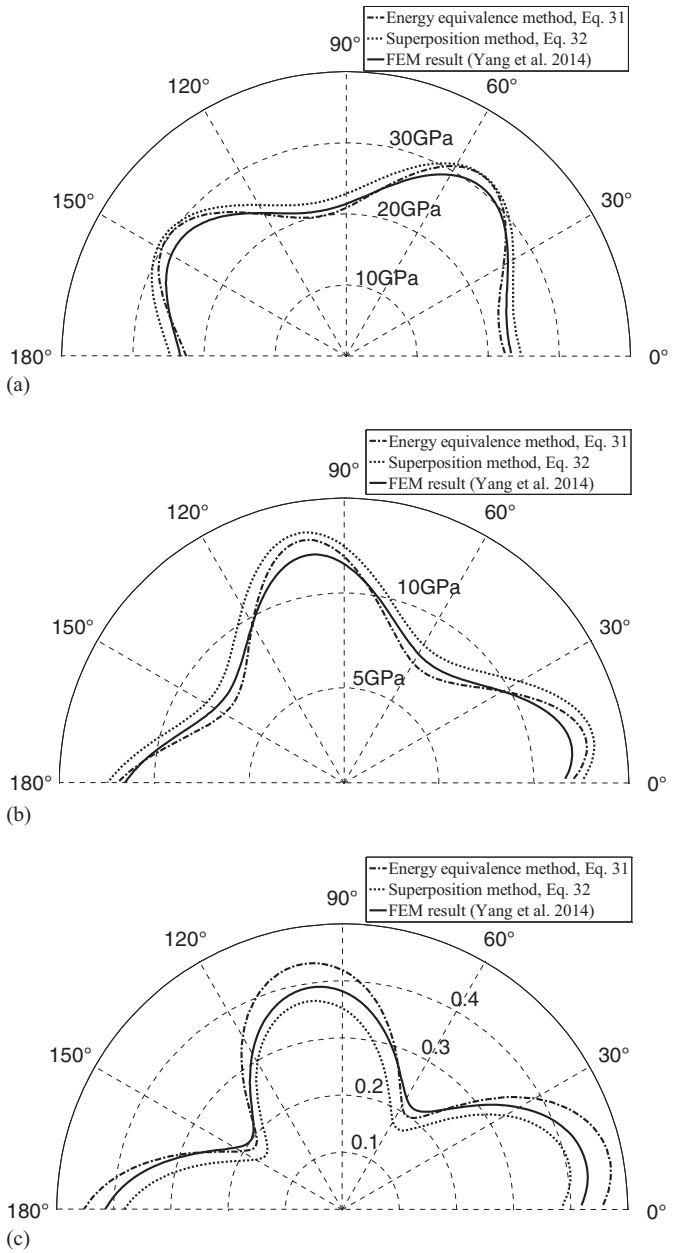

Fig. 9. Comparison of elastic constants between analytical and FEM modeling results: (a) Young's modulus (in gigapascals); (b) shear modulus (in gigapascals); (c) Poisson's ratio

Summary and Conclusion

1. The energy equivalence method was adopted to estimate the compliance matrix of a fractured rock mass in which the stiffness of nonpersistent fractures was incorporated. Two loading schemes were proposed to determine the components of S_{16} and S_{26} for nonsymmetric fracture sets. The derived compliance matrix was consistent with the closed-form expression (Huang et al. 1995; Amadei and Goodman 1981) for regular persistent fracture sets, and it agreed well with the FEM modeling results for normally distributed nonpersistent fracture sets.
2. In the present study, the displacement jumps of a nonpersistent fracture are different from the previous analytical studies. Normal

and shear stiffnesses are considered to be related with the displacement jumps [Eq. (5)]. This fracture constitutive relationship has been widely used in numerical simulations (Kulatilake et al. 1993; Min and Jing 2003; Esmaieli et al. 2010; Wu and Kulatilake 2012; Khani et al. 2013) but has not been adopted in an analytical study. It is noteworthy that the formula of a fracture displacement jump significantly influences the format of the compliance matrix. For example, Oda et al. (1984) obtained a compliance matrix in which $S_{12} = S_{13} = S_{23}$ and $S_{16} = S_{26}$ according to the assumption that the jump vector was parallel to the traction vector. However, these constraints may not hold if the adopted fracture jump formula changes. It is, therefore, suggested that reasonable fracture jumps for different kinds of discontinuities (bedding planes, joints, fissures) and rock types should be determined before deriving a rock mass compliance matrix.

3. In addition to the energy equivalence method and strain average method, a superposition method was proposed. The equivalent compliance matrix of rock masses containing several sets of persistent, nonpersistent, or mixed types of fractures can be roughly estimated using the superposition method through the superposition of the elementary compliance matrices of intact rock (S_{int} in Fig. 4), persistent fracture set [Eq. (25)], and the derived nonpersistent fracture set [Eq. (27)]. It is noteworthy that the superposition method ignores the fracture interaction effects between different fracture sets.
4. The simplified fracture model adopted in the analytical work does not take into account the complexity of the real fracture shape (Zhang and Einstein 2010), nonlinearity of fracture-deformation behavior (Bandis et al. 1983), or shear dilation of real fractures. The constant fracture stiffnesses assumed in this paper can be used with a small load increment and give approximate estimations for a large load increment (Huang et al. 1995). The derived expressions will be improved in the future to estimate the compliance matrix of a rock mass in the nonelastic range.

Appendix

Determination of Compliance Matrix by Energy Equivalent Method

Determination of S_{11}

Loading Set 1 is activated. According to the theory of linear elasticity (Brady and Brown 2013), the elastic-strain energy density stored in the equivalent elastic body is

$$\bar{U}_1 = \frac{\sigma}{2}\varepsilon_{xx} = \frac{\sigma^2}{2}S_{11} \tag{33}$$

The elastic-strain energy density determined, following the theory of fracture mechanics [Eqs. (6) and (7)], is

$$U_1 = \frac{\sigma^2}{2E_0} + \sum_{i=1}^{N}\rho_i \Delta\Sigma_{i,\text{loadingset1}}$$
$$= \frac{\sigma^2}{2E_0} + \frac{\sigma^2}{4}\sum_{i=1}^{N}\rho_i \pi a_i^2 \cdot \left[\frac{(1+\cos 2\theta_{ix})^2}{K_n \pi a_i + E_{\perp i}} + \frac{\sin^2 2\theta_{ix}}{K_s \pi a_i + E_{\| i}}\right] \tag{34}$$

where $\Delta\Sigma_{i,\text{loadingset1}}$ = increment of strain energy due to the presence of a single fracture of the ith fracture set under Loading Set 1 in Fig. 2. The value of $\Delta\Sigma_{i,\text{loadingset1}}$ is calculated from Eq. (6), by resolving the far-field stress, σ, into the normal stress, σ_n, and shear stress, τ_s, on the fracture plane, and θ_{ix} is the angle between the x-axis and the normal direction of ith fracture set.

Combining Eqs. (33) and (34), component S_{11} can be solved with Eq. (11).

Determination of S_{22}

Loading Set 2 is activated. The elastic-strain energy density stored in the equivalent elastic body is

$$\bar{U}_2 = \frac{\sigma}{2}\varepsilon_{yy} = \frac{\sigma^2}{2}S_{22} \tag{35}$$

The elastic-strain energy density, determined using the theory of fracture mechanics, is

$$U_2 = \frac{\sigma^2}{2E_0} + \sum_{i=1}^{N}\rho_i \Delta\Sigma_{i,\text{loadingset2}}$$
$$= \frac{\sigma^2}{2E_0} + \frac{\sigma^2}{4}\sum_{i=1}^{N}\rho_i \pi a_i^2 \cdot \left[\frac{(1+\cos 2\theta_{iy})^2}{K_n \pi a_i + E_{\perp i}} + \frac{\sin^2 2\theta_{iy}}{K_s \pi a_i + E_{\| i}}\right] \tag{36}$$

Combining Eqs. (35) and (36), component S_{22} can be solved with Eq. (12).

Determination of S_{66}

Loading Set 3 is activated. The elastic-strain energy density stored in the equivalent elastic body is

$$\bar{U}_3 = \tau\varepsilon_{xy} = S_{66}\tau^2 \tag{37}$$

The elastic-strain energy density, determined following the theory of fracture mechanics [Eqs. (6) and (9)], is

$$U_3 = \frac{\tau^2}{2G_0} + \sum_{i=1}^{N}\rho_i \Delta\Sigma_{i,\text{loadingset3}}$$
$$= \frac{\tau^2}{2G_0} + \tau^2\sum_{i=1}^{N}\rho_i \pi a_i^2 \cdot \left(\frac{\sin^2 2\theta_{iy}}{K_n \pi a_i + E_{\perp i}} + \frac{\cos^2 2\theta_{iy}}{K_s \pi a_i + E_{\| i}}\right) \tag{38}$$

Combining Eqs. (37) and (38), component S_{66} can be solved with Eq. (13).

Determination of S_{12}

Loading Sets 1, 2, and 4 are activated. The elastic-strain energy density stored in Loading Set 4 is

$$\bar{U}_4 = \frac{\sigma}{2}(\varepsilon_{xx} + \varepsilon_{yy}) = \frac{S_{11} + S_{12} + S_{21} + S_{22}}{2}\sigma^2 \tag{39}$$

The difference between $\bar{U}_1 + \bar{U}_2$ and $\bar{U}_4$ is

$$\bar{U}_1 + \bar{U}_2 - \bar{U}_4 = -S_{12}\sigma^2 \tag{40}$$

Furthermore, the strain-energy density difference can be calculated as

$$U_1 + U_2 - U_4 = \frac{\nu_0}{E_0}\sigma^2 + \sum_{i=1}^{N}\rho_i \cdot \left(\Delta\Sigma_{i,\text{loadingset1}} + \Delta\Sigma_{i,\text{loadingset2}} - \Delta\Sigma_{i,\text{loadingset4}}\right) = \frac{\nu_0}{E_0}\sigma^2 + \frac{\sigma^2}{4}\sum_{i=1}^{N}\rho_i \pi a_i^2 \cdot \left[\frac{(1+\cos 2\theta_{ix})^2}{K_n \pi a_i + E_{\perp i}} + \frac{\sin^2 2\theta_{ix}}{K_s \pi a_i + E_{\parallel i}} + \frac{(1+\cos 2\theta_{iy})^2}{K_n \pi a_i + E_{\perp i}} + \frac{\sin^2 2\theta_{iy}}{K_s \pi a_i + E_{\parallel i}} - \frac{4}{K_n \pi a_i + E_{\perp i}}\right] \quad (41)$$

Combining Eqs. (40) and (41), component S_{12} can be solved with Eq. (14).

Determination of S_{16}

Loading Sets 1, 3, and 5 are activated. The elastic-strain energy density stored in Loading Set 5 is

$$\bar{U}_5 = \frac{1}{2}\sigma\varepsilon_{xx} + \tau\varepsilon_{xy} = \frac{1}{2}\left(S_{11}\sigma^2 + S_{16}\sigma\tau + 2S_{61}\sigma\tau + 2S_{66}\tau^2\right) \quad (42)$$

The difference between $\bar{U}_1 + \bar{U}_3$ and $\bar{U}_5$ is

$$\bar{U}_1 + \bar{U}_3 - \bar{U}_5 = -S_{16}\sigma\tau \quad (43)$$

Furthermore, the strain-energy density difference can be calculated as

$$U_1 + U_3 - U_5 = \sum_{i=1}^{N}\rho_i \cdot \left(\Delta\Sigma_{i,\text{loadingset1}} + \Delta\Sigma_{i,\text{loadingset3}} - \Delta\Sigma_{i,\text{loadingset5}}\right) = \sigma\tau \cdot \sum_{i=1}^{N}\rho_i \pi a_i^2 \cdot \left[\frac{(1+\cos 2\theta_{ix}) \cdot \sin 2\theta_{iy}}{K_n \pi a_i + E_{\perp i}} - \frac{\cos 2\theta_{iy} \cdot \sin 2\theta_{ix}}{K_s \pi a_i + E_{\parallel i}}\right] \quad (44)$$

Combining Eqs. (43) and (44), component S_{16} can be solved with Eq. (15).

Determination of S_{26}

Loading Sets 2, 3, and 6 are activated. Compared to Loading Set 5, the only difference is attributed to the resolved normal and shear stresses on the fracture surface. Therefore, S_{26} is obtained with Eq. (16).

Acknowledgments

The authors gratefully acknowledge the support of the Chinese Fundamental Research (973) Program, through Grants 2015CB057900 and 2013CB03600, and the support of the National Natural Science Foundation of China (Grants 51225902, 51004097, and 51309217).

References

Agharazi, A., Martin, C. D., and Tannant, D. D. (2012). "A three-dimensional equivalent continuum constitutive model for jointed rock masses containing up to three random joint sets." *Geomech. Geoeng.*, 7(4), 227–238.

Amadei, B., and Goodman, R. E. (1981). "A 3-D constitutive relation for fractured rock masses." *Proc., Int. Symp., Mechanical Behavior of Structured Media*, A. P. S. Selvadurai, ed., Part B, Elsevier Scientific, New York, 249–268.

Bandis, C. S., Lumsden, A. C., and Barton, N. R. (1983). "Fundamentals of rock joint deformation." *Int. J. Rock Mech. Min. Sci. Geomech. Abstr.*, 20(6), 249–268.

Barton, N. (2002). "Some new Q-value correlations to assist in site characterisation and tunnel design." *Int. J. Rock Mech. Min. Sci.*, 39(2), 185–216.

Bieniawski, Z. T. (1978). "Determining rock mass deformability: Experience from case histories." *Int. J. Rock Mech. Min. Sci. Geomech. Abstr.*, 15(5), 237–247.

Brady, B. H. G., and Brown, E. T. (2013). *Rock mechanics: For underground mining*, George Allen & Unwin, London.

Budiansky, B., and O'Connell, R. J. (1976). "Elastic moduli of a cracked solid." *Int. J. Solids Struct.*, 12(2), 81–97.

Cai, M., and Horii, H. (1992). "A constitutive model of highly jointed rock masses." *Mech. Mater.*, 13(3), 217–246.

Chen, S. H., He, J., and Shahrour, I. (2012). "Estimation of elastic compliance matrix for fractured rock masses by composite element method." *Int. J. Rock Mech. Min. Sci.*, 49(Jan), 156–164.

Esmaieli, K., Hadjigeorgiou, J., and Grenon, M. (2010). "Estimating geometrical and mechanical REV based on synthetic rock mass models at Brunswick Mine." *Int. J. Rock Mech. Min. Sci.*, 47(6), 915–926.

Goodman, R. E., Taylor, R. L., and Brekke, T. L. (1968). "A model for the mechanics of jointed rock." *J. Soil Mech. and Found. Div.*, 94(3), 637–660.

Gutierrez, M., and Youn, D.-J. (2015). "Effects of fracture distribution and length scale on the equivalent continuum elastic compliance of fractured rock masses." *J. Rock Mech. Geotech. Eng.*, 7(6), 626–637.

Hoek, E., and Diederichs, M. S. (2006). "Empirical estimation of rock mass modulus." *Int. J. Rock Mech. Min. Sci.*, 43(2), 203–215.

Horii, H., and Nemat-Nasser, S. (1983). "Overall moduli of solids with microcracks: Load-induced anisotropy." *J. Mech. Phys. Solids*, 31(2), 155–171.

Hu, K. X., and Huang, Y. (1993). "Estimation of the elastic properties of fractured rock masses." *Int. J. Rock Mech. Min. Sci.*, 30(4), 381–394.

Huang, T. H., Chang, C. S., and Yang, Z. Y. (1995). "Elastic moduli for fractured rock mass." *Rock Mech. Rock Eng.*, 28(3), 135–144.

Irwin, G. R. (1957). "Analysis of stresses and strains near the end of a crack traversing a plate." *J. Appl. Mech.*, 24, 361–364.

Kachanov, M. (1993). "Elastic solids with many cracks and related problems." *Adv. Appl. Mech.*, 30, 259–445.

Kachanov, M. L. (1982). "A microcrack model of rock inelasticity part I: Frictional sliding on microcracks." *Mech. Mater.*, 1(1), 19–27.

Kemeny, J., and Cook, N. G. W. (1986). "Effective moduli, non-linear deformation and strength of a cracked elastic solid." *Int. J. Rock Mech. Min. Sci. Geomech. Abstr.*, 23(2), 107–118.

Khani, A., Baghbanan, A., and Hashemolhosseini, H. (2013). "Numerical investigation of the effect of fracture intensity on deformability and REV of fractured rock masses." *Int. J. Rock Mech. Min. Sci.*, 63(Oct), 104–112.

Kim, B. H., Cai, M., Kaiser, P. K., and Yang, H. S. (2007). "Estimation of block sizes for rock masses with non-persistent joints." *Rock Mech. Rock Eng.*, 40(2), 169–192.

Kulatilake, P. H. S. W., Wang, S., and Stephansson, O. (1993). "Effect of finite size joints on the deformability of jointed rock in three dimensions." *Int. J. Rock Mech. Min. Sci. Geomech. Abstr.*, 30(5), 479–501.

Li, C. (2001). "A method for graphically presenting the deformation modulus of jointed rock masses." *Rock Mech. Rock Eng.*, 34(1), 67–75.

Min, K.-B., and Jing, L. (2003). "Numerical determination of the equivalent elastic compliance tensor for fractured rock masses using the distinct element method." *Int. J. Rock Mech. Min. Sci.*, 40(6), 795–816.

Oda, M., Suzuki, K., and Maeshibu, T. (1984). "Elastic compliance for rock-like materials with random cracks." *Soils Found.*, 24(3), 27–40.

Palmström, A., and Singh, R. (2001). "The deformation modulus of rock masses—comparisons between in situ tests and indirect estimates." *Tunnelling Underground Space Technol.*, 16(2), 115–131.

Sonmez, H., Gokceoglu, C., and Ulusay, R. (2004). "Indirect determination of the modulus of deformation of rock masses based on the GSI system." *Int. J. Rock Mech. Min. Sci.*, 41(5), 849–857.

Wang, T.-T., and Huang, T.-H. (2009). "A constitutive model for the deformation of a rock mass containing sets of ubiquitous joints." *Int. J. Rock Mech. Min. Sci.*, 46(3), 521–530.

Wu, Q., and Kulatilake, P. H. S. W. (2012). "REV and its properties on fracture system and mechanical properties, and an orthotropic constitutive model for a jointed rock mass in a dam site in China." *Comput. Geotech.*, 43(Jun), 124–142.

Yang, J.-P., Chen, W.-Z., Dai, Y.-h., and Yu, H.-D. (2014). "Numerical determination of elastic compliance tensor of fractured rock masses by finite-element modeling." *Int. J. Rock Mech. Min. Sci.*, 70(Sep), 474–482.

Yang, J. P., Chen, W. Z., Yang, D. S., and Tian, H. M. (2016). "Estimation of elastic moduli of non-persistent fractured rock masses." *Rock Mech. Rock Eng.*, 49(5), 1977–1983.

Zhang, L., and Einstein, H. H. (2004). "Using RQD to estimate the deformation modulus of rock masses." *Int. J. Rock Mech. Min. Sci.*, 41(2), 337–341.

Zhang, L., and Einstein, H. H. (2010). "The planar shape of rock joints." *Rock Mech. Rock Eng.*, 43(1), 55–68.